Lithium Insertion in Three-Dimensional Tin Sulfides

I. Lefebvre* and M. Lannoo

IEMN, ISEN department, 41, Boulevard Vauban, 59046 Lille Cedex, France

M. Elidrissi Moubtassim, J. Olivier Fourcade, and J.-C. Jumas

LPMS, Université Montpellier II, Place Eugène Bataillon, 34095 Montpellier Cedex 5, France

Received March 7, 1997. Revised Manuscript Received September 23, 1997[⊗]

The tin reduction during lithium insertion in spinel sulfide compounds is investigated. Mössbauer and RMN spectroscopy are combined with tight binding calculations to analyze the reduction mechanism. It is shown that the formal reaction $Sn^{IV} + 2e^- \rightarrow Sn^{II}$ is involved without an intermediate Sn oxidation state. The following mechanism is proposed: lithium ions create shallow and deep-defect donor states; the trapping of two electrons on the deep one, which exhibits a negative *U* behavior, induces the reduction of the corresponding tin atom.

The insertion of a guest species G as a G^+ ion and an electron e^- in a host material ⟨H⟩ is generally associated with a transfer of electron density and an oxido-reduction reaction which is written under the form

$$\langle H\rangle + xG^+ + xe^- \leftrightarrows \langle G_xH\rangle$$

These insertion compounds ⟨H⟩ have many potential applications such as electrodes in solid-state batteries.[1] The most currently studied materials have lamellar structures[2,3] (such as graphite or transition-metal sulfides) as they provide space and preferential diffusion paths for small particles and thus offer the possibility to realize easy and reversible reactions. Nevertheless, interest in three-dimensional network host materials has also been raised,[4] particularly when the insertion leads to only one solid phase and is reversible. Among these materials, the spinel type compounds seem to be promising low-potential electrodes.[5,6] Such "one-phase solid redox compounds" have been isolated in the In_2S_3−XS−SnS_2 system, where X stands for Sn, Fe, or Cu. In this system, a solid-state region has been defined where mixed valence X sulfides are based on the spinel form of In_2S_3.[7,8] These spinel sulfides are three-dimensional and characterized by the presence of vacancies and the possibility for X atoms to adopt two oxidation states (Sn^{II-IV}, Fe^{II-III}, or Cu^{I-II}) which correspond to different electronic configurations. Up to now, the lithium insertion has been analyzed in the spinel tin indium sulfides with the help of various experimental techniques.[9,10] As deduced from X-ray diffraction spectroscopy, the reaction

$$\langle InSnS\rangle + xLi^+ + xe^- \leftrightarrows \langle Li_xInSnS\rangle$$

occurs without structural change. Atomic emission spectroscopy has been used to measure the inserted lithium quantity and has shown that the insertion is nearly reversible. The ^{7}Li nuclear magnetic resonance spectrum has shown that lithium atoms are introduced in the spinel sulfides under ionic form.

During Li insertion, Sn^{IV} atoms (formal electronic configuration $4d^{10}$) are supposed to be reduced into Sn^{II} (formal electronic configuration $4d^{10}5s^2$) through the reaction $Sn^{IV} + 2e^- \rightarrow Sn^{II}$ where the two electrons are supplied by two inserted lithium atoms. ^{119}Sn Mössbauer spectroscopy, which gives information on the electronic distribution around tin atoms, shows that only part of the Sn^{IV} atoms are reduced resulting in two distinct situations Sn^{IV} and Sn^{II} with no intermediate oxidation state between the two. The conventional view however would assume that the band structure of the host material remains unchanged under insertion and that electrons supplied by Li are filling the conduction bands, simply changing the Fermi level position (rigid band model). In this picture, the number of s electrons on Sn would vary continuously from its Sn^{IV} value to Sn^{II}, leading to intermediate oxidation states that are not observed.

Our aim here is to explain this discrepancy by an analysis of the electronic transfer during the insertion and to propose an original mechanism for the reduction of host species. We choose $In_{16}Sn_4S_{32}$ as a representative compound because it contains only Sn^{IV} atoms (no Sn^{II}) before insertion, and thus the reduction effect is more significant. In section I, we introduce the tight-binding method used here to calculate the electronic

[⊗] Abstract published in *Advance ACS Abstracts,* November 15, 1997.

(1) Wittingham, M. S. *MRS Bull.* **1989**, *Sept.* 31.
(2) Wittingham, M. S.; Jacolison, A. J. *Intercalation chemistry*; Academic Press: New York, 1982.
(3) Wiegers, G. A.; Meetsma, A.; Van Smaalen, S.; Haange, R. J.; Wulff, J.; Zeinstra, Th. J.; De Boer, J. L.; Kuypers, S.; Van Tendeloo, G.; Van Landuyts, J.; Amelinckx, S.; Meersschaut, A.; Rabu, P.; Rouxel, J. *Solid State Comm.* **1989**, *70*, 409.
(4) Uchida, T.; Tanjo, Y.; Wakihara, M.; Tanaguchi, M. *J. Electrochem. Soc.* **1990**, *137*, 7.
(5) Ferg, E.; Gummow, R. J.; Thackeray, M. M.; de Kock, A. *J. Electrochem. Soc.* **1994**, *141*, 11.
(6) Gummow, R. J.; de Kock A.; Thackeray, M. M. *Solid State Ionics* **1994**, *69*, 59.
(7) Moralès, J.; Tirado, J. L.; Elidrissi-Moubtassim, M. L.; Fourcade, J.; Jumas, J. C. *J. Alloys Compounds* **1995**, *217*, 176.
(8) Cochez, M. A.; Jumas, J.−C.; Lavela, P.; Moralès, J.; Olivier-Fourcade, J.; Tirado, J. L. *J. Power Sources* **1996**, *62*, 101.
(9) Elidrissi-Moubtassim, M. L.; Jumas, J.−C. *Eur. J. Solid State Inorg. Chem.* **1991**, *28*, 1307.
(10) Elidrissi-Moubtassim, M. L.; Jumas, J.−C.; Senegas, J. *J. Solid State Chem.* **1990**, *87*, 1.

S0897-4756(97)00139-7 CCC: $14.00

structures. As we are dealing with the tin reduction, the chemical notion of tin oxidation state is analyzed in section II. The third section is devoted to the electronic structure of $In_{16}Sn_4S_{32}$ which is calculated by using two approaches: (i) the full tight-binding method, which gives densities of states, and (ii) tight-binding molecular models to obtain a simplified description. In section IV, the insertion and tin reduction mechanism are analyzed in terms of the electronic structure. We treat lithium ions as point defects and show that they induce deep or shallow donor states in the gap according to the insertion site. We demonstrate that the deep donor state is unstable under local atomic distortions and exhibits negative *U* behavior. We thus end up with a collection of either doubly occupied or empty donor states. This situation explains the complete reduction of some tin atoms, while the others remain in their Sn^{IV} form.

I. Tight-Binding Method

The band structure calculations are performed in order to obtain the total and partial densities of states and electronic populations. Due to the complex atomic structure of the spinel sulfides, we have used the empirical tight-binding (TB) method, whose simplicity allows a full calculation. It is a well-documented procedure[11] which has already given good results for such complex compounds.[12−15] The TB description is based on the use of a s−p minimal basis set consisting of one s and three p atomic orbitals $\varphi_{i\alpha}$ (where *i* stands for the atom and α for the orbital index) which correspond to the external valence states. The wave function is expressed as a linear combination of these orbitals (LCAO approximation). The energy levels *E* are given by the secular equation:

$$\mathrm{Det}|H - ES| = 0 \qquad (1)$$

where the Hamiltonian *H* and the overlap matrix *S* are written in the minimal basis set. In the TB approximation, *S* is taken as the unit matrix. The calculation of the energy levels requires the knowledge of the Hamiltonian matrix elements where the diagonal ones are the atomic energies and the others the hopping integrals. We consider the two-center approximation which allows to express these hopping integrals in terms of four nonvanishing independent terms:

$$H_{\alpha\beta}(i,j) = H_{ss}(i,j),\ H_{s\sigma}(i,j),\ H_{\sigma s}(i,j),\ H_{\sigma\sigma}(i,j),\ H_{\pi\pi}(i,j) \qquad (2)$$

defined for a pair of atoms (*i*,*j*) and orbitals $\alpha\beta$; s stands for s orbitals, σ and π for p orbitals respectively along and perpendicular to the (*i*,*j*) axis. They are parametrized with the empirical law:

$$H_{\alpha\beta}(i,j) = \eta_{\alpha\beta}\frac{\hbar^2}{m}\frac{1}{\sum ij^2}\exp\left(-2.5\left(\frac{d}{\sum ij} - 1\right)\right) \qquad (3)$$

where $\sum ij$ is the sum of the *i* and *j* atomic radii *R*,[16] *d* is the interatomic distance, and $\eta_{\alpha\beta}$ are empirically defined coefficients.[17] We take the intraatomic terms to be diagonal and equal to free atom energies tabulated by Herman and Skillman.[11] All these parameters are reported in Table 1.

Table 1. Tight-Binding Parameters[a]

	In	Sn	S
R	1.56	1.45	0.88
E_s	−10.12	−12.50	−20.80
E_p	−4.69	−5.95	−10.27
η_{ss}	$\eta_{s\sigma}$	$\eta_{\sigma\sigma}$	$\eta_{\pi\pi}$
−1.32	1.42	2.22	−0.63

[a] *R* are atomic radii (in Å)[16] and E_s, E_p the atomic levels (in eV)[11] for the concerned atoms. $\eta_{\alpha\beta}$ are the interatomic parameters[17] used in eq 3.

To perform the full TB calculation, we take advantage of Bloch's theorem, which reduces the problem to the diagonalization of a $4N \times 4N$ matrix for each **k** vector in the reciprocal space (*N* is the number of atoms per unit cell). To understand the chemical bonding, we determine the total and partial densities of states (DOS and PDOS). The energies $E(\mathbf{k})$ are calculated for "special **k** points" in the Brillouin zone,[18] and each level is broadened by convolution with a Gaussian of width 0.25 eV. To analyze the difference between Sn^{II} and Sn^{IV} and the evolution of the Fermi level during insertion, we also have to calculate partial electron populations on each atomic state $\varphi_{i\alpha}$, given by

$$N_{i,\alpha} = 2\sum_{n,k} f_{n,k}|\langle\varphi_{i,\alpha}|\Psi_{n,k}\rangle|^2 \qquad (4)$$

where $\Psi_{n,k}$ is the Bloch state of vector *k* belonging to band *n* and $f_{n,k}$ is the occupancy factor (equal to 1 for filled bands and 0 for empty ones). The total number of electrons in the cell is $\sum_{i,\alpha}N_{i,\alpha}$.

II. Tin Oxidation State

Our interest in this paper is the formal tin reduction reaction $Sn^{IV} + 2e^- \rightarrow Sn^{II}$, where the oxidation state is changing from IV to II. Let us first discuss the change in local electronic properties associated to this reaction from the study of various tin sulfides compounds selected in the $In_2S_3-SnS-SnS_2$ family.[19] The formal oxidation state is defined as the net charge (in units of e) that the atom would have if its bonds were treated in the purely ionic limit, i.e., if all the electrons of a bond were assigned to the most electronegative element. The neutral Sn electronic configuration is $4d^{10}5s^25p^2$. Its oxidation configurations would thus be $4d^{10}5s^2$ for Sn^{II} and $4d^{10}$ for Sn^{IV}. This corresponds to what is observed in ^{119}Sn Mössbauer spectra (Figure 1) which only present two peak positions for this family of compounds.

(11) Harrison, W. A. *Electronic Structure and Properties of Solids;* Freeman: San Francisco, 1980.
(12) Lefebvre, I.; Lannoo, M.; Allan, G.; Ibanez, A.; Olivier-Fourcade, J.; Jumas, J. C.; and Beaurepaire, E. *Phys. Rev. Lett.* **1987**, *59*, 2471.
(13) Lefebvre, I.; Lannoo, M.; Allan, G.; Martinage, L. *Phys. Rev. B* **1988**, *38*, 8593.
(14) Sferco, S. J.; Allan, G.; Lefebvre, I.; Lannoo, M.; Bergignat, E.; Hollinger, G. *Phys. Rev. B* **1990**, *42*, 11232.
(15) Albanesi, E. A.; Sferco, S. J.; Lefebvre, I.; Allan, G.; Hollinger, G. *Phys. Rev. B* **1992**, *46*, 13260.
(16) Clementi, E.; Raimondi, D. L.; Reinhardt, W. P. *J. Chem. Phys.* **1967**, *47*, 1300.
(17) Harrison, W. A. *Phys. Rev. B* **1981**, *24*, 5835.
(18) Chadi, D. J.; Cohen, M. L. *Phys. Rev. B* **1973**, *8*, 5747.
(19) Lefebvre, I.; Lannoo, M.; Olivier-Fourcade, J.; Jumas, J. C. *Phys. Rev. B* **1991**, *44*, 1004.

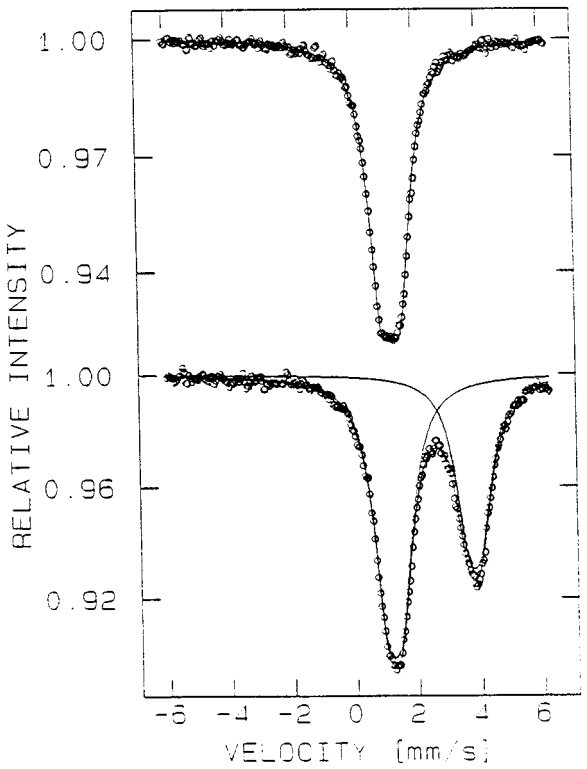

Figure 1. ^{119}Sn Mössbauer spectra for $In_{16}Sn_4S_{32}$ before (a) and after (b) lithium insertion.

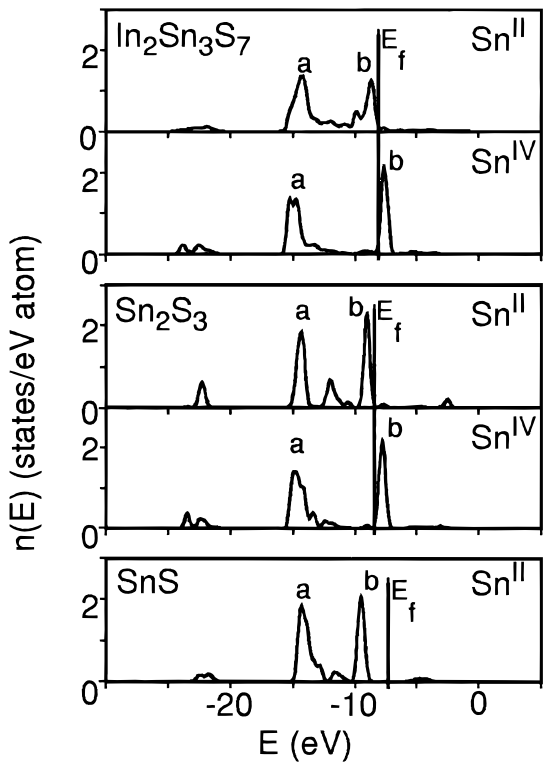

Figure 2. Partial density of states for the various tin sulfides. Ef is the Fermi level position.

The corresponding isomer shift parameter δ[20] can be written as

$$\delta = K(|\Psi_m(0)|^2 - |\Psi_r(0)|^2) \quad (5)$$

where the prefactor K depends only on nuclear terms, $|\Psi(0)|^2$ is the electronic density at the nucleus, and the m, r subscripts stand for measured and reference materials. As $|\Psi(0)|^2$ is proportional to the 5s(Sn) population and the reference material is the same in all cases, the isomer shift variation ($\Delta\delta$) between two oxidation states is then

$$\Delta\delta = K\Delta n_s \quad (6)$$

where K is a constant and Δn_s stands for the difference between the 5s(Sn^{IV}) and 5s(Sn^{II}) population. The experimental peak positions $\delta \approx 1.1$ mm/s and $\delta \approx 3.5$ mm/s are attributed to the existence of Sn^{IV} and Sn^{II} atoms (an intermediate position is observed in the covalent materials such as αSn where the s(Sn) character is expected to be intermediate).

In ref 19 we have calculated the electronic structure of various compounds belonging to the $In_2S_3-SnS-SnS_2$ system, chosen in order to present various situations for tin atoms: distorted local environment or symmetrical ones, mixed or single valence ones. We have obtained a good agreement between the theoretical densities of states and the photoemission spectra when available. The same technique has been used to calculate the tin electronic population, which is reported in Table 2. We mainly conclude that the 5s(Sn) electron population (n_s) is the driving parameter to define the tin oxidation state. One notices that n_s essentially takes two values: $n_s = 1.2$ for Sn^{IV} and $n_s = 1.9$ (which corresponds to the lone pair) for Sn^{II} although a larger spread of values occurs for the total population. As discussed in ref 19 this difference in 5s population ($\Delta n_s \approx 0.7$) quantitatively reproduces via eq 6 (with the appropriate value of K) the experimental values of the Mössbauer isomer shift ($\Delta\delta \approx 2.4$ mm/s) and corresponds to the partial 5s(Sn) densities of Figure 2. These densities are characterized by two peaks where the lowest in energy is always in the valence band and the upper one is either in the valence band for Sn^{II}, either in the conduction band for Sn^{IV}. The important point here is that no intermediate situation is possible for the 5s(Sn) density in this type of compounds. This kind of conclusion has also been pointed out for the Ga and As oxidation state in other materials.[15]

Table 2. For the Various Chosen Compounds, δ Is the Experimental ^{119}Sn Mössbauer Isomer Shift, n(5s+5p) Is the Calculated Number of Tin Electrons, and n(5s) Is the Calculated Number of 5s Tin Electrons

	Sn^{IV}			Sn^{II}		
	δ (mm/s)	n(5s)	n(5s+5p)	δ (mm/s)	n(5s)	n(5s+5p)
SnS_2	1.13	1.22	2.69			
$In_2Sn_3S_7$	1.19	1.25	2.54	3.82	1.92	2.88
SnS				3.31	1.94	3.00
Sn_2S_3	1.16	1.18	2.48	3.53	1.92	3.00
$In_{16}Sn_4S_{32}$	1.16	1.20	2.50			

In this family of sulfides, tin oxidation states are also shown to be related to the local atomic environment around Sn atoms. For Sn^{II}, the distorted environments with Sn−S distances varying from 2.5 up to 3.5 Å correspond to the lone-pair (ns = 1.9 electron) activity. Concerning Sn^{IV} atoms, the environments present an octahedral geometry with Sn−S distances close to 2.6 Å, like in $In_{16}Sn_4S_{32}$.

III. Electronic Structure of $In_{16}Sn_4S_{32}$

We are dealing here with tin sulfides based on the spinel structure. We have chosen to study the In_{16}-

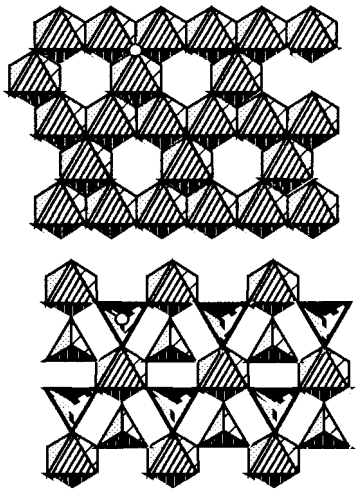

Figure 3. $In_{16}Sn_4S_{32}$ crystallographic structure showing the stacking of layers. When they are superposed, the white circles are in coincidence.

Table 3. Possible Crystallographic Sites in the Spinel Structure[a]

site name	8a	16d	8b	16c	48f
occupancy	In, □	In, Sn	Li, □	Li, □	Li, □
polyhedron	tetra	octa	tetra	octa	tetra
d(X−S)	2.452	2.606	2.188	2.757	2.328
d(X−Sn)			2.320	3.789	2.365

[a] The first line gives the site name, the second one their possible occupancy by atoms or vacancies □, the third one indicates the kind of sulfur polyhedron on which they are centered (tetrahedra or octahedra), d(X−S) is the average distance between the site center X and the sulfur neighbors (expressed in Å), and d(X−Sn) the distance between X and the nearest tin atoms.

Sn_4S_{32} compound as its ^{119}Sn Mössbauer spectrum (Figure 1a) presents only one peak at position $\delta = 1.16$ mm/s corresponding to the oxidation state IV for tin atoms.

$In_{16}Sn_4S_{32}$ crystallizes in the spinel form. The structure may be described as the stacking of two layers: the first one made by sulfur octahedra sharing edges (Figure 3a), the other made by sulfur tetrahedra sharing tops with octahedra (Figure 3b) of the same layer and of the upper or lower layer, to achieve the stacking. Its detailed formula is $(In_4,□_4)[In_{12},Sn_4]S_{32}$ where □ is a vacancy site, ( ) stands for sites at the center of sulfur tetrahedra and [ ] for sites at the center of sulfur octahedra (Table 3). Thus, the centers of tetrahedra are partially filled and vacancies are randomly distributed on these sites. Concerning the centers of the octahedra, indium and tin atoms are also randomly distributed.

The tight-binding calculations give the total and partial densities of states (DOS) drawn on Figure 4. The theoretical forbidden bandgap (2.5 eV) compares well with the experimental one (2.1 eV). One must here notice that the upper 5s(Sn) peak density is at the bottom of the conduction band. The electronic 5s(Sn) population is reported in Table 2. These theoretical results are in agreement with an oxidation state IV for the Sn atoms.

It is interesting for what follows to qualitatively describe this electronic structure without any numerical calculation. For doing this, the compound is understood in regards to its atomic structure and the nature of the chemical bonds (covalent character or not). The point

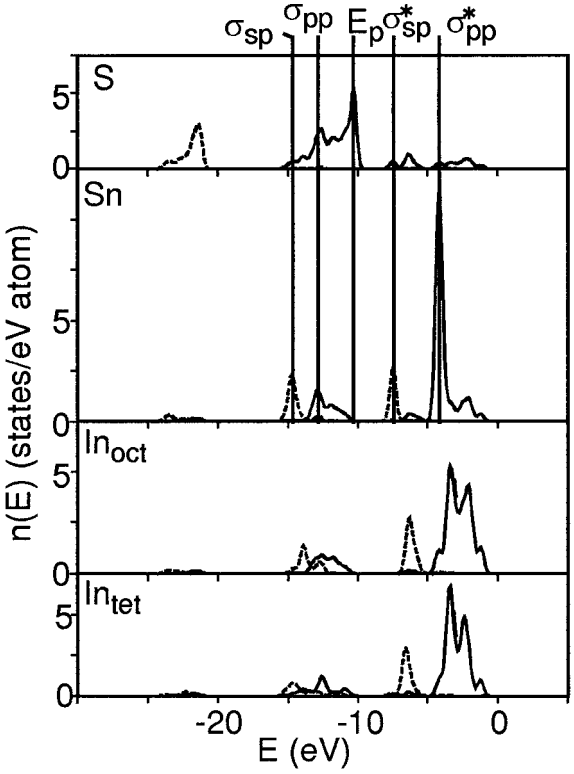

Figure 4. $In_{16}Sn_4S_{32}$ theoretical partial density of states: p character in straight line, s character in dotted line.

is to idealize the structure in order to obtain a set of molecular units, if possible. The method is based on the TB description and on a suitable basis change such that the Hamiltonian matrix is dominated by elements corresponding to the main chemical bonds. Then, the other elements are neglected in the model, leading to a description of the electronic structure as it gets highly degenerate levels. The inclusion of further interactions will broaden these levels into bands, as is the case in the full TB calculation.

Let us now construct the $In_{16}Sn_4S_{32}$ molecular model. Its atomic structure has been described as the stacking of sulfur octahedra and sulfur tetrahedra. We first consider that these units are disconnected. As far as we are concerned with tin atoms, we then describe the electronic structure of SnS_6 perfect octahedral units. We denote α(A) the atomic orbital of symmetry α which is centered on atom A. The Sn atom has one s state and three p states. There is one p(S) orbital per sulfur atom which points toward Sn (i.e., with his positive lobe in the Sn direction). We also consider the interatomic terms $\langle p(S)|H|p(Sn)\rangle = \beta_{pp}$ and $\langle p(S)|H|s(Sn)\rangle = \beta_{sp}$. The SnS_6 molecular model (Figure 5) is characterized by the following features:

(i) The s(S) state has a deep atomic level (Table 1) and is thus assumed to remain uncoupled.

(ii) In a given direction (x for example), the Hamiltonian matrix is written in the basis

$$\{p_x(Sn),\ (p_x(S1) - p_x(S2))/\sqrt{2},\quad (p_x(S1) + p_x(S2))/\sqrt{2}\}$$

$$[H] = \begin{bmatrix} E_p(Sn) & \beta_{pp}\sqrt{2} & 0 \\ \beta_{pp}\sqrt{2} & E_p(S) & 0 \\ 0 & 0 & E_p(S) \end{bmatrix} \qquad (7)$$

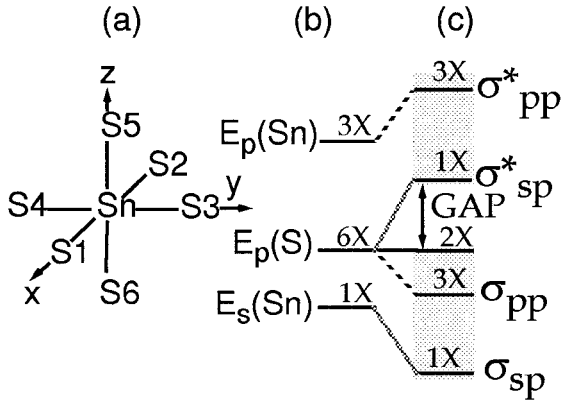

Figure 5. $In_{16}Sn_4S_{32}$ molecular model: (a) octahedral unit centered on Sn atom, (b) atomic level position, (c) molecular levels.

It gives rise to a bonding state σ_{pp} at the energy $E_{pp} = E^a_{pp} - \sqrt{\delta_{pp}{}^2+2\beta_{pp}{}^2}$ and an antibonding state σ^*_{pp} at the energy $E^*_{pp} = E^a_{pp} + \sqrt{\delta_{pp}{}^2+2\beta_{pp}{}^2}$, where $E^a_{pp} = (E_p(Sn) + E_p(S))/2$ and $\delta_{pp} = (E_p(Sn) - E_p(S))/2$. The energy states values are −12.03 eV for σ_{pp} and −4.18 eV for σ^*_{pp} as indicated by the arrows on the partial sulfur densities in Figure 4. This situation also occurs for the *y* and *z* axes, leading to a triple degeneracy for these states. Thus the p(Sn) population in the σ_{pp} state is equal to

$$3 \times 2 \times \frac{1}{2}\left[1 - \frac{\delta^2}{\sqrt{\delta_{pp}^2 + 2\beta_{pp}^2}}\right] = 1.349$$

which value is close to the fully calculated one of 1.306 electrons.

(iii) The interaction between the s(Sn) and p(S) states gives rise, in the basis $\{s(Sn), (p_x(S1) + p_x(S2) + p_y(S3) + p_y(S4) + p_z(S5) + p_z(S6))/\sqrt{6}\}$ to the Hamiltonian matrix:

$$[H] = \begin{bmatrix} E_s(Sn) & \beta_{sp}\sqrt{6} \\ \beta_{sp}\sqrt{6} & E_p(S) \end{bmatrix} \qquad (8)$$

whose eigenvalues are $E_{sp} = E^a_{sp} - \sqrt{\delta_{sp}{}^2+6\beta_s{}^2{}_p}$ for the bonding σ_{sp} state and $E^*_{sp} = E^a_{sp} + \sqrt{\delta_{sp}{}^2+6\beta_s{}^2}$ for σ^*_{sp} with $E^a_{sp} = (E_s(Sn) + E_p(S))/2$ and $\delta_{pp} = (E_p(S) - E_s(Sn))/2$. Their respective energies (−15.18 and −7.58 eV) are reported on the densities drawn in Figure 4. This model gives extremely precise values for the s(Sn) population. While filling the bonding states, the number of s(Sn) electrons in the valence band is

$$n_s = 1 + \frac{\delta_{sp}}{\sqrt{\delta_{sp}{}^2 + 6\beta_{sp}{}^2}} \qquad (9)$$

whose value 1.29 is very close to the fully calculated one (1.20).

Concerning indium atoms, the octahedral InS_6 molecules will give the same scheme as the SnS_6 units above-described, with nearly the same molecular energies as the In and Sn atomic levels are comparable. The situation between the In tetrahedral and octahedral units should be exactly the same provided that the interaction terms (which appears in eq 8) $\beta\sqrt{N} = \beta_0\sqrt{N}\ \exp(-2.5(d/\Sigma ij - 1))$ are the same (N is the number of sulfur atoms, d the interatomic distance, and Σij the sum of atomic radii). This equality leads to a required variation in interatomic distance between octahedral and tetrahedral sites $d_6 - d_4 = 0.189$ Å, which compares well with 0.154 Å given by X-ray spectroscopy. The densities of states are thus nearly the same, as shown in Figure 4.

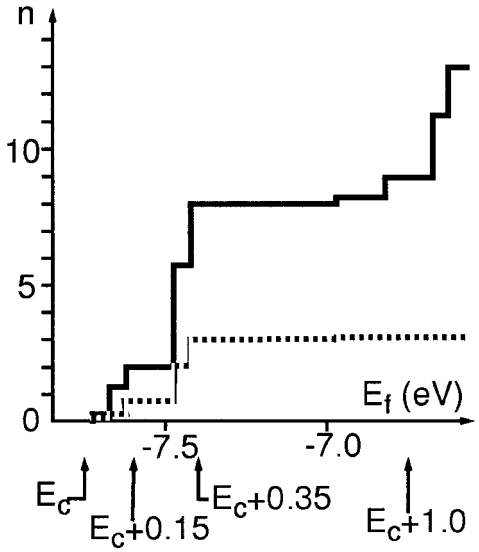

Figure 6. Total number of electron in a unit cell (straight line) and partial s(Sn) one (dotted line) in the conduction band as a function of the Fermi level position.

As will be explained in the next section, the character of the bottom of the conduction band is of great importance in interpreting the reduction mechanism. Let us now describe its main features. From partial densities of states and molecular models, the conduction band below −7.40 eV only involves s(Sn) and p(S) states. Figure 6 presents the evolution of the total number of electrons in a unit cell and the partial s(Sn) one in the conduction band as a function of the Fermi level position (E_f). It clearly shows that for E_f between −7.4 and −7.0 eV, there are only four states containing a total of 8 electrons. This energy range corresponds to the σ^*_{sp} molecular states whose number is 4 per unit cell. In this model, the addition of n electrons in the conduction band leads to an increase Δn_s of s(Sn) population:

$$\Delta n_s = \frac{n}{2}\left(1 - \frac{\delta_{sp}}{\sqrt{\delta_{sp}{}^2 + 6\beta_{sp}{}^2}}\right) \qquad (10)$$

whose value $\Delta n_s = 0.35n$ is in good agreement with the full calculation corresponding to Figure 6 which gives $\Delta n_s = {}^3/_8 n = 0.375n$. In fact, the molecular model can even describe the fine structure of Figure 6. Indeed each of the four molecular σ_{sp}* antibonding states of the unit cell can be written in the form

$$\Psi = \alpha\, \varphi_{s,\,Sn} - \sqrt{1-\alpha^2}\, \varphi_{p,\,S} \qquad (11)$$

where $\varphi_{s,Sn}$ is one s(Sn) atomic state, $\varphi_{p,S}$ the combination of the sulfur neighbors leading to eq 8, and $\alpha = \sqrt{0.38}$. A weak interaction between the four SnS_6 units will slightly lift the degeneracy of these states. This fact is clearly observable in Figure 6 with two plateaus of weight two and six, corresponding to one state at nearly $E_c + 0.15$ eV and three degenerate states

around $E_c + 0.35$ eV their center of gravity lying at $E_{cg} = E_c + 0.30$ eV.

In conclusion of this part, the main features of the band structure are identified by the molecular model which then gives a correct description of the chemical bonding in such a spinel structure. The population of the states is also quantitatively well reproduced.

IV. Lithium Insertion

As shown in Figure 3, there exist in the spinel structure many interstitial crystallographic sites (Table 3) where the Li may be placed. After insertion, the ^{119}-Sn Mössbauer spectrum (Figure 1b) is built of two peaks: one at nearly the same position as before (Sn^{IV}), the new one at $\delta = 3.70$ mm/s showing the presence of Sn^{II}, due to the reduction of Sn^{IV}. A detailed analysis of the Mössbauer spectra confirms the position in octahedral sites for Sn^{IV} as well as for Sn^{II}. It is important here to point out that only part of the tin atoms are reduced, and all of them have the same δ value. The X-ray diffraction spectroscopy is in agreement with a topotactic reaction, i.e., a reaction that occurs without structural change and shows that the lithium atoms are randomly placed in the structure. Finally, the chemical shift of the ^{7}Li NMR signal ($\nu_0 = 77.7$ MHz) indicates that the Li atoms are ionically introduced. An analysis of the NMR central line shows that Li^+ ions are inserted in both octahedral and tetrahedral sites.

The excess electrons provided by the ionization of the Li atoms are donated to the host atoms. In most known inserted systems the presence of the Li^+ ions cores does not modify substantially the host band structure. In such a scheme the excess electrons should gradually fill the lowest conduction band as described by Figure 6. This means that one would obtain for all the tin atoms the same situation with the possibility of intermediate oxidation states (n_s between 1.2 and 1.9 electrons per tin atom). Thus this rigid band model does not correctly describe the experimental observation of either Sn^{IV} ($n_s = 1.2$) or Sn^{II} ($n_s = 1.9$). The real mechanism has at least to create different situations between the reduced and unreduced tin atoms.

A first possibility is to consider the Li^+ disorder effect, which induces long-range potential fluctuations. If these are of macroscopic size, the conduction bands will follow this potential fluctuation rigidly. The excess electrons filling the conduction band, the Fermi level position E_f defines the tin oxidation states. When $E_c(\vec{r})$, the bottom of the conduction band at position $(\vec{r})$, is above E_f, the tin atoms are not reduced. When E_f is greater than $E_c(\vec{r}) + 0.35$ eV (Figure 6), Δn_s equals 0.7 electron and the tin atoms situated in the corresponding regions are reduced. However, there remain some topographic zones where E_f stands between these limits, again leading to intermediate oxidation states. Their quantity will be negligible if the amplitude of the fluctuation is large. We have made the calculation using a Gaussian probability distribution and found that these intermediate states should be detectable, ruling out this explanation.

A second possibility is the formation of lithium clusters. To estimate the maximum possible effect, we consider a spherical cluster in which the Li^+ ions fill all insertion sites and spread out the charge uniformly in the sphere. This gives rise to an attractive potential that can capture electrons. We find that the self-consistent solution gives the Fermi level position at the cluster center as

$$E_f - E_c = -0.3 N_{Li}^{2/3} \text{ eV} \qquad (12)$$

where N_{Li} is the total number of lithium atoms in a cluster. However, near the cluster boundary, tin atoms are again in an intermediate oxidation state, and their quantity will be negligible only if N_{Li} is fairly large. But such clusters are not observed, and the only solution is to deal with isolated lithium ions.

IV.1. Lithium Impurities. We now analyze the lithium as an impurity that can introduce donor energy levels in the forbidden bandgap of the perfect crystal. The easiest thing to do first is to treat it as a shallow donor, making use of effective mass theory.[21] In this way we get the usual series of hydrogenic states below the conduction, the binding energy in the lowest 1s state being

$$E_b = 13{\cdot}6 m^*/\epsilon^2 \text{ eV} \qquad (13)$$

and the corresponding Bohr radius

$$a^* = 0.53\epsilon/m^* \qquad (14)$$

To calculate these quantities, we first estimate the effective mass m^* from Figure 6 by using the following free electron relation:

$$m^* = \left(\frac{3\pi^2 N(E_f - E_c)}{\Omega}\right)^{2/3} \frac{\hbar^2}{2(E_f - E_c)} \qquad (15)$$

where $N(E_f - E_c)$ is the number of electrons from E_c to E_f and Ω the unit cell volume ($(20.226)^3$ atomic units). From Figure 6, the $N(E_f - E_c = 1$ eV) value is nearly 10 electrons leading to $m^* = 1.47$ atomic units. With the experimental dielectric constant $\epsilon = 10$, eq 13 gives a binding energy $E_b = 0.2$ eV, which is larger than the typical ones and a Bohr radius $a^* = 3.6$ Å which is quite smaller than the unit cell parameter so that the effective mass theory does not apply and the defect has to be understood as a deep defect. Nevertheless, E_b is much less than the forbidden gap (2.1 eV), and one may thus consider that it corresponds to a localized state whose wave function is built from the states at the bottom of the conduction band.[21]

Such states have been studied in section III, where we have demonstrated that the bottom of the conduction band is built from the individual state Ψ defined by eq 11. Each such state can be stabilized when it experiences the attractive potential of a nearby Li^+ atom, and it will have a lower energy. This can lead to a deep level whose wave function will be close to Ψ. This localized state may trap an electron, and the increase in 5s(Sn) population is then depending on the Ψ character which

(20) Janot, C. *L'effet Mössbauer et ses applications*; Masson and Cie: Paris, 1972.

(21) Lannoo, M.; Bourgoin, J. *Point defects in Semiconductors I; Theoretical aspects*; Springer-Verlag: Berlin, 1981.

is partly s(Sn). The interest here is that this variation in 5s character occurs only for the tin atom concerned by the localized state. To study this, we have used the two approaches (molecular model and full tight binding).

IV.2. Donor Binding Energies due to Li^+ Ions. Let us first consider the molecular model. We again have to deal with the SnS_6 octahedral molecule. The Coulomb potential due to a Li^+ ion at some distance R is $-e^2/\epsilon R$. It will be applied to the Sn and S atoms. The energy of the lowest state Ψ then becomes

$$E = E_{cg} + \alpha^2\left(-\frac{e^2}{\epsilon R}\right) + (1-\alpha^2)\frac{1}{6}\sum_{i=1}^{6}\left(-\frac{e^2}{\epsilon R_i}\right) \quad (16)$$

where E_{cg} stands for the average energy of Ψ before perturbation by the Li^+ potential (E_c + 0.3 eV), R the Li^+-Sn distance, and R_i the Li^+-S ones. To a very good approximation $\sum_i 1/R_i \sim 6/R$ so that the level position corresponding to (16) can be written:

$$E_b = E_{cg} - e^2/\epsilon R \quad (17)$$

Different cases have now to be considered. There exist different insertion sites for a given Sn atom (see Table 3), the closest being at nearly 2.3 Å, a further one lying at 3.8 Å. These two cases lead to distinct one-electron level positions: $E = E_c - 0.33$ eV for "close" sites or $E = E_c - 0.1$ eV for "distant" sites. Of course there are even more distant sites, but they would lead to levels practically degenerated with E_c or even within the conduction band.

To confirm these conclusions, we have performed full calculations using a periodic cell technique, with one Li^+ per unit cell, this one being centered on the Li^+ insertion site. Even if this leads to artificial defect−defect interactions, the size of our unit cell (52 atoms + 4 vacancy sites) is large enough for this effect to be small. The potential $-e^2/\epsilon R$ is applied to each atom of the unit cell with R the real distance between Li^+ and the considered atom. This term is then added to the atomic energy in order to constitute the new diagonal terms in the Hamiltonian matrix. The results of this full calculation are represented in Figure 7. It is first clear that for "close" $Sn-Li^+$ pairs, an energy level appears in the bandgap. One may also observe that the band limits also weakly vary since the diagonal Hamiltonian elements have changed. This induces corrections to the binding energy. For the close pair, conduction and valence band limit are shifted to lower energies by 0.14 and 0.25 eV, respectively. When the correction for E_c is applied, the true donor level position will thus be $E_c = -0.38$ eV close to the molecular model value. Concerning the distant pair, the defect level cannot be isolated from the conduction band in agreement with the smaller binding energy (∼0.1 eV) found in the molecular model.

One may summarize the obtained situation as follows: lithium ions create deep and shallow localized states depending on their position relative to tin atoms. Each one may trap an electron, but in this case, the variation in 5s population on the corresponding Sn atom depends on Ψ (eq 11) and may be written as

$$\Delta n_s = \alpha^2 = 0.38 \quad (18)$$

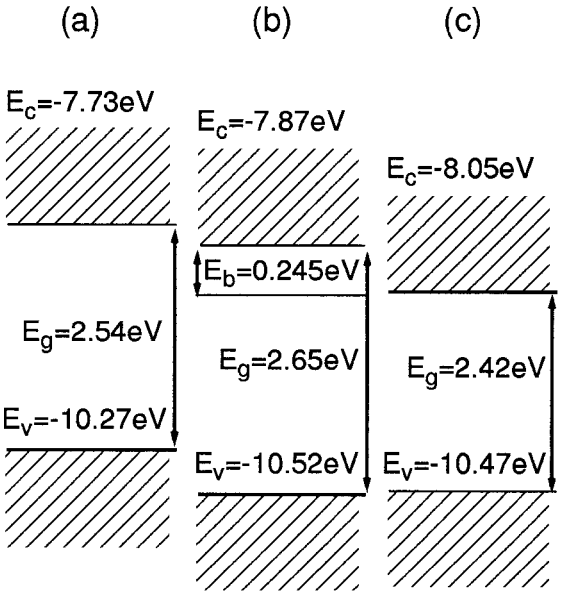

Figure 7. Energy schemes obtained from full calculation where E_c stands for the lowest conduction energy, E_v for the upper valence band one and E_b the one electron binding energy. They present the following situations: perfect host (a) and inserted one with Li "close" from one tin atom (b) and "far" from one tin atom (c).

This value is not sufficient to transform Sn^{IV} into Sn^{II}, which would require $\Delta n_s \sim 0.7$. Such a situation could be realized only with two electrons in the deep state. However, due to the Coulomb repulsion between the two electrons, it is not clear whether such a negatively charged donor state is stable. The object of the next section is then to calculate the effective value of the Coulomb term.

IV.3. Effective *U* Calculation. The effective U is built from two contributions: (i) U_{ee}, the direct Coulomb repulsion between the two electrons; (ii) U_R, the relaxation part due to the change in lattice configuration with increasing electron population on the donor level. As discussed in ref 21, the Coulomb repulsion between two electrons, each in the state Ψ with opposite spin is given by

$$U_{ee} = \frac{e^2}{\epsilon}\int \frac{|\Psi(1)|^2|\Psi(2)|^2}{r_{12}}\,d\tau_1\,d\tau_2 \quad (19)$$

A first simple estimation is provided by the hydrogenic picture, since it is known from results on H and H^- that in such a case $U_{ee} \approx E_B$, the binding energy in the neutral state. Transposing this equality to the present situation would lead to $U_{ee} \sim 0.2$ eV in the pure hydrogenic picture of section IV.1 and to $U_{ee} \sim 0.38$ eV for the deep-level calculation of section IV.2.

Another estimate is obtained by using the molecular description of Ψ given by eq 11:

$$U_{ee} = (1/\epsilon)\{\alpha^4 U_{Sn,Sn} + (1-\alpha^2)^2 U_{S,S} + (1-\alpha^2)\alpha^2 U_{Sn,S}\} \quad (20)$$

where $U_{i,j}$ is the Coulomb term between an electron on atom i and the other on atom j. To take into account the reduction of U_{ee} due to correlation effects, we calculate (20) with the assumption that when an electron sits on one site, the other one is as far as

possible. Thus, one obtains

$$U_{\mathrm{Sn,S}} \approx \frac{1}{6}\sum_{i=1}^{6} U_{\mathrm{Sn,\,S}_i} = e^2/\epsilon R$$

$$U_{\mathrm{Sn,Sn}} \approx e^2/\epsilon R$$

$$U_{\mathrm{S,S}} = (1/6^2)\sum_{i,j} e^2/\epsilon R_{ij} \approx e^2/2\epsilon R \qquad (21)$$

where in the second term $U_{\mathrm{Sn,Sn}}$ is replaced by $U_{\mathrm{Sn,S}}$ and in the third one, $U_{\mathrm{S,S}}$, each R_{ij} is given its largest value $2R$, with R the Sn−S distance. These approximations lead to $U_{\mathrm{ee}} = 0.44$ eV, which probably is a slight overestimate since Ψ should become slightly more delocalized when going beyond the molecular model. Anyway such a value is close to the second one, 0.38 eV, given before so that a fair estimate should be $U_{\mathrm{ee}} \sim$ 0.4 eV.

We now have to evaluate the relaxation term U_{R}. For doing this, let us first remind the notion of occupancy level[21] and various expressions of the energy. The total energy of a point defect can be labeled as $E_{\mathrm{t}}(n,R_{\mathrm{n}})$ since it depends upon the number n of electrons in the gap state and the corresponding equilibrium nuclear configuration R_{n}. The occupancy level $E(n+1, n)$ is defined as

$$E(n+1, n) = E_t(n+1, \boldsymbol{R}_{n+1}) - E_t(n, \boldsymbol{R}_n) \qquad (22)$$

The position of the Fermi level with respect to $E(n+1, n)$ determines if the state is filled ($n+1$ electrons) or empty (n electrons). In section IV, we have already calculated $E(1,0)$ characterizing the ionized ($n = 0$) and neutral ($n = 1$) states but without allowing for lattice relaxation. To know if the deep center will capture two electrons, we have to calculate $E(2,1)$ and $E(1,0)$ including the lattice relaxation contribution. The effective Coulomb term is the difference between these two occupancy levels

$$U_{\mathrm{eff}} = E(2,1) - E(1,0) \qquad (23)$$

It can be expressed under the form:

$$U_{\mathrm{eff}} = U_{\mathrm{ee}} + U_R \qquad (24)$$

where U_{ee} is the pure electronic part discussed before, U_{R} corresponding to the lattice relaxation contribution.

To evaluate the total energies and relaxations, we first calculate the electronic structure of $In_{16}Sn_4S_{32}$ by the use of the density functional theory in the local density approximation (calculations have been realized using the code of ref 22). The obtained theoretical structure presents no gap irrespective of convergence requirements. Such a situation is well-known for LDA results for many semiconductors. It avoids its use in studying localized states as is here our aim. Thus total energies and relaxations are calculated within the tight-binding technique, introducing new parameters with the ability to accurately reproduce total energy variations with atomic displacements are checked on simpler tin sulfides within the LDA (as will be shown later).

Within the tight-binding technique, the total energy E_{t} of the host can be expressed as $E_{\mathrm{t}} = E_{\mathrm{bs}} + E_{\mathrm{r}}$, where the band structure energy E_{bs} is defined by the sum over all occupied states $E_j(\mathbf{k})$ with wave vector $\mathbf{k}$ and band index j:

$$E_{\mathrm{bs}} = 2\sum_{k,j} E_j(k) \qquad (25)$$

and E_{r} is a repulsive energy. In total energy TB calculations, this one is often modelized by a Born−Mayer potential:

$$E_r = \sum_{ab} C_{a-b} \exp\left(-\mathrm{p}\left(\frac{\mathrm{d}}{\sum ab} - 1\right)\right) \qquad (26)$$

with d the interatomic distance and $C_{\mathrm{a}-b}$ a prefactor constant between atom a and b. This kind of expression has been successfully used for sp elements and transition metals,[23] and the p value is generally considered as twice as large as that occurring in the electronic interactions given by eq 3. We retain such a value here, i.e., $p = 5$.

In a first step we calculate the relaxation contribution to U from the molecular model. As the SnS_6, InS_6 octahedra, and InS_4 tetrahedra are weakly linked, we independently consider a breathing mode relaxation of an SnS_6 unit (each bond length in the unit is axially increased by the same quantity u) in the perfect host. In this model, the total energy in the molecular model is written as

$$E_{\mathrm{t}}^0 = E_{\mathrm{s}}(\mathrm{Sn}) + 3E_p(\mathrm{Sn}) + 8E_{\mathrm{p}}(\mathrm{S}) - 2\sqrt{\delta_{\mathrm{sp}}{}^2 + 6\beta_{\mathrm{sp}}{}^2} - 6\sqrt{\delta_{\mathrm{pp}}{}^2 + \beta_{\mathrm{pp}}{}^2} + 6C_{\mathrm{Sn-S}} \qquad (27)$$

with the notations of section III. Knowing that the β decay is $\exp(-qu)$ and that the $C_{\mathrm{Sn-S}}$ one is $\exp(-pu)$ with $p/q = 2$, the equilibrium condition (cancelation of the first derivative of the total energy) leads to

$$2\mathrm{q}\left\{\frac{6\beta_{\mathrm{sp}}{}^2}{\sqrt{\delta_{\mathrm{sp}}{}^2 + 6\beta_{\mathrm{sp}}{}^2}} + 3\frac{\beta_{\mathrm{pp}}{}^2}{\sqrt{\delta_{\mathrm{pp}}{}^2 + \beta_{\mathrm{pp}}{}^2}}\right\} = 6pC_{\mathrm{Sn-S}} \qquad (28)$$

We can inject $C_{\mathrm{Sn-S}}$ obtained by (28) into the second derivative $\mathrm{d}^2E_t^0/\mathrm{d}u^2$ deduced from (27) which gives the force constant k. Its numerical calculation leads to a value $k = 20.47$ eV/Å^2. We can also perform the corresponding full calculation (with the exact numerical band structure energy) for the same kind of distortion of the SnS_6, InS_6, and InS_4 units. Thus the fully calculated force constant value for the SnS_6 unit turns out to be $k = 21.78$ eV/Å^2, in excellent agreement with the value deduced from the molecular model.

This force constant may characterize the Sn−S bond. A test of our tight-binding parameter ($C_{\mathrm{Sn-S}}$) is realized by a DFT−LDA calculation of k for SnS_2, which has been chosen in the $SnS-In_2S_3-SnS_2$ family because it exhibits the same octahedral sulfur environment around Sn^{IV} as in $In_{16}Sn_4S_{32}$. The Sn−S distance in SnS_2 (2.56 Å) is also similar to those in $In_{16}Sn_4S_{32}$ (2.60 Å). The k value has been calculated for two kinds of basis set: (i) a pseudopotential representation of the ions and a plane

(22) *DSolid 4.0.0 User Guide*; MSI: San Diego, 1996. *Plane-Wave 4.0.0 User Guide*; MSI: San Diego, 1996).

(23) Allan, G.; Lannoo, M. *J. Phys. (Paris)* **1983**, *44*, 1355.

Table 4. Total Energy E_t (in eV) for the Relaxation u_S and u_{Sn} (in Å) in the Occupancy State n and Relaxation Contribution U_R (in Å)

model	n	E_t	u_S	u_{Sn}	U_R
molecular	0		0.00		
	1		0.18		−0.67
	2		0.36		
first full calculated	0	−3653.42	0.0		
	1	−3661.06	0.1		−0.59
	2	−3669.29	0.3		
improved full calculated	0	−3653.27	0.0	0.2	
	1	−3661.27	0.1	0.1	−0.60
	2	−3669.87	0.2	0.2	

[a] Results are given for the molecular model, the full calculated one constructed to check the molecular one, and the full calculated model which takes all effects into account.

wave expansion for the wave functions, which gives $k_{DFT,\ ps} = 19.5$ eV/Å^2 and (ii) a numerical atomic basis given on an atomic-centered spherical−polar mesh, which gives $k_{DFT,\ nu} = 23.4$ eV/Å^2. This range of values, as compared to the previous one, $k = 21.78$ eV/Å^2, allows us to consider that our set of TB parameters is capable of quantitatively describing the lattice response around Sn to the electrostatic force induced by the Li^+ ion.

Let us now deal with the inserted material in the molecular model and consider the localized level given by eq 17 whose wave function is the antibonding state Ψ expressed by eq 11. If we put n extra electrons in this state, the change in energy can be written, to second order in u, as

$$E_t(n,u) = E_t(n,u=0) + nFu + {}^1/_2 ku^2 \qquad (29)$$

where $Et(n,u=0)$ is obtained from E_t^0 by adding the energy of n electrons in the antibonding level. We can determine F from the first derivative of $E_t(n,u)$:

$$F = q6\beta_{sp}{}^2/\sqrt{\delta_{sp}{}^2 + 6\beta_{sp}{}^2} \qquad (30)$$

which gives the value $F = 3.72$ eV/Å. To simplify, we take the value of k given by E_t^0 which introduces little error. We now have all the tools for an evaluation of the relaxation. The new equilibrium situation corresponding to (29) is

$$u = \frac{F}{k}n$$

$$E_t(n, R_n) = E_t(n, u = 0) - \frac{F^2}{2k}n^2$$

From (23) we get the repulsive part of U_{eff}: $U_R = -F^2/k^2$. With our numerical values of F and k, we find $U_R = -0.67$ eV (Table 4). The effect is substantial and the effective U_{eff} is then negative (+0.40 − 0.67 = −0.27 eV). However, the molecular model neglects the interactions with the other cells, which when taken into account might modify this result.

We have thus performed the corresponding full numerical calculation to check this result. As in the molecular model described above, we do not include the electrostatic interactions due to the Li^+ ion core. However, to simulate the corresponding effect, we artificially put an attractive potential on the central Sn atom with enough strength (2.0 eV) to stabilize the correct gap

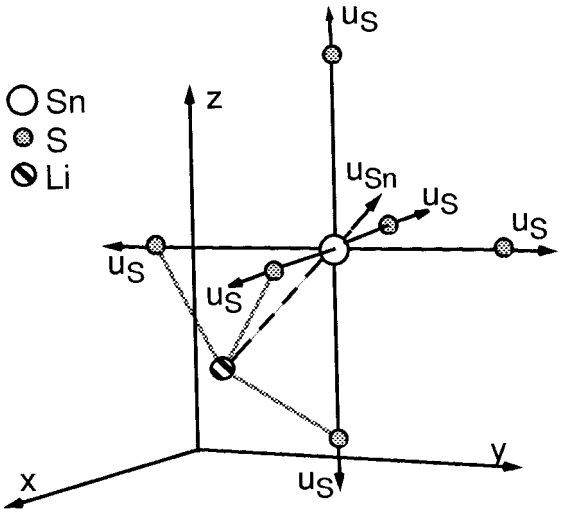

Figure 8. Relaxation of the SnS_6 molecule due to the lithium defect.

state which is then filled with $n = 0, 1, 2$ electrons. We then calculate the total band structure energies, add the repulsive pair potentials adjusted to reproduce the correct bulk bond lengths and minimize the total energy $E_t(n,u)$. The numerical results are given in Table 4 (full calculation 1) and compare fairly well with the molecular model, confirming its essential validity.

We now discuss a much more complete calculation including Li^+ electrostatic effects and allowing for distortions of the SnS_6 octahedron.

IV.4. Refined Insertion Model. The previous model may be improved by consideration of two effects that have been neglected in the previous calculation:

(1) It is necessary to include the electrostatic interactions induced by the Li^+ ion core. These are determined in a point-charge approximation $-qe^2/\epsilon d$, where d is the distance from Li^+ and q is the charge in units of the electron charge.

(2) The change in atomic configuration of the SnS_6 unit has been assumed up to now to correspond to a breathing relaxation with only an increase of the Sn−S bonds. We also have to consider the possibility of a displacement of the Sn atom along the Li−Sn axis (u_{Sn} parameter) opposite to the Li (Figure 8). This is now a distortion that might correspond to the solid-state chemistry notion which as the stereochemical activity of the $5s^2$ lone pair as we hope to obtain this lone pair ($n_s = 1.9$) on the reduced tin.

Thus the total energy is $E_t = E_{bs} + E_r + E_{Li}$, where E_{bs} and E_r are the previously defined band structure and repulsive energies, while E_{Li} is the electrostatic energy due to the Li^+ core. We now have all the tools to evaluate the total energy and to study the relaxation by minimizing E_t, for varying defect occupancy ($n = 0$, 1, 2), with respect to the two lattice displacements u_S (breathing) and u_{Sn} (distortion).

Final results are presented in Table 4. From the definitions (22) and (23), the component of the shift in energy of the occupancy level due to relaxation when it captures an electron is $U_R = -0.60$ eV. This confirms that the effective U_{eff} is really negative ($U_{eff} = 0.40 - 0.60 = -0.20$ eV). This means that the two occupancy levels $E(2,1)$ and $E(1,0)$ are inverted with respect to their normal ordering $E(2,1) > E(1,0)$ which would correspond to a positive electron−electron repulsion.

This is by now a well-established situation for point defects in semiconductors.[24] A particularly interesting consequence of this inversion is that, from statistics, it can be shown that the level can only either be completely filled (2 electrons) or completely empty. The "filled" case, according to our calculation, corresponds to 1.9 electrons on Sn, i.e., the situation characteristic of Sn^{II}.

Until now, we have only dealt with the deeper center, i.e., the case of a lithium ion inserted "near" a particular tin atom. The case of the shallower defects (where the lithium is inserted further from the tin atom) is a bit different. In this case, the Li^+ is outside the SnS_6 octahedra and, as we have seen, could at best lead to a fairly shallow donor level. We have not found any possibility that these situations could lead to gap levels competing with those of the "deep" case analyzed in detail before. We are thus led to the conclusion that such levels are, for our purpose, always above those of the closer pair.

Conclusion

In this study, we have based our investigations in order to agree with the main experimental evidence about the insertion of lithium atoms in spinel−tin−sulfide compounds: (i) RMN spectra show that lithium atoms are ionically introduced; (ii) Mössbauer spectra show that some Sn^{IV} atoms are reduced to Sn^{II} and that no intermediate situation occurs. This evidence leads us to consider lithium ions as point defects, and their effect on the electronic structure is calculated by a full tight-binding method as well as tight-binding molecular levels. We have then demonstrated that donor states are induced and that the deep one, which is unstable under local atomic distortion, exhibits a negative *U* behavior.

One may thus sum up the reduction mechanism of one tin atom as follows:

(1) A Li^+ atom is inserted "near" Sn_1. It provides one electron in a deep donor state.

(2) Another Li^+ is inserted "far" from Sn_2. It creates a shallower level and provides a second electron.

(3) This second electron is then trapped by the first deep level Sn_1, leading to a more stable situation and increasing the $s(Sn_1)$ electronic character to about 1.9 electrons. Thus the Sn_1 is completely reduced according to the well-known chemical relation: $Sn^{IV} + 2e^- \rightarrow Sn^{II}$, which requires the insertion of two lithium atoms for the reduction of one tin atom.

CM970139H

(24) Anderson, P. W. *Phys. Rev. Lett.* **1975**, *34*, 953. Baraff, G. A.; Kane, E. O.; Schluter, M. *Phys. Rev. Lett* **1979**, *43*, 956; *Phys. Rev. B* **1980**, *21*, 3583.